

## Research Article

# The Immittance Response of Escherichia Coli Bacteria

Mohammad A Alim<sup>1\*</sup>, Sudip Bhattacharjee<sup>2</sup> and Josh Herring<sup>3</sup>

<sup>1</sup>Department of Electrical Engineering and Computer Science, Alabama A & M University, P.O. Box 297 Huntsville, Alabama 35762, USA

<sup>2</sup>Department of Mechanical and Civil Engineering, Alabama A & M University, P.O. Box 367 Huntsville, Alabama 35762, USA

<sup>3</sup>Department of Food and Animal Science, Alabama A & M University, P.O. Box 1628 Huntsville, Alabama 35762, USA

\*Corresponding author: Mohammad A Alim, Department of Electrical Engineering and Computer Science, Alabama A & M University, P.O. Box 297 Huntsville, Alabama 35762, USA

Received: November 08, 2014; Accepted: November 20, 2014; Published: November 21, 2014

## Abstract

In this study the *ac* small-signal electrical data are obtained for the sterile *BHI* and *E. Coli* bacteria suspended *BHI* material systems to extract an equivalent circuit model via Bode plot in conjunction with the complex plane plot. It is observed that the non-blocking conductive nature of the underlying operative electrical paths between the two opposite electrodes across the sample (material system) exist satisfying *dc* condition of the equivalent circuit model. Thus, the proposed equivalent circuit model verifies the existence of the shunt resistance that provides a meaningful representation of the material system. The non-Debye behavior is not addressed as this work is emphasized to establish correct equivalent circuit model.

**Keywords:** E. Coli; Impedance; Immittance; Bode plot; Equivalent circuit model

## Introduction

The *brain heart infusion (BHI)* broth based material system used as a medium for the *Escherichia coli (E. Coli)* bacteria growth has been investigated [1, 2] via impedance or admittance (immittance) measurements to determine underlying operative mechanisms. The immittance measurement provides a powerful tool to understand the detection process of *E. Coli* as well as the total behavior of the same in the suspended medium. In order to detect bacteria, relative or absolute changes in the constituting immittance parameters are used [3]. The electrical response of the bacterial behavior is ascertained by specific pattern of the data display and subsequent proposition of the equivalent circuit model [5-14].

The *ac small-signal data* when displayed in the complex plane formalisms [15-20] the underlying conduction processes between the two electrodes across the material system is delineated for the operative phenomena. This display supports traditional Bode plot and thus, does not violate the general requirements of the elements constituting the equivalent circuit model. The advantage of the complex plane plot is that an equivalent circuit model can easily be extracted unless dual representation of the complex plane plot of the same data is observed. Semicircular relaxation achieved in more than one complex plane provides at least one reasonable operative equivalent circuit. This has been demonstrated for a number of solid state material systems [21-30]. The sterile and bacterial media give rise to equivalent circuit model comprising of the simplistic series *R-C* (resistive-capacitive) combination [1-14]. This type of equivalent circuit model is blocking in nature that prohibits the flow of direct current (*dc*). The immittance data generation for a variety of peak-to-peak voltages indicates that there is no existence of the blocking element prohibiting the flow of *dc* through the material system. Invariably the *dc* condition can be extrapolated from the convenient Bode plot [15-17].

The *ac* electrical measurements and complex plane plotting

techniques are used to establish operative mechanisms via representative equivalent circuit model for the material system regardless of the state. Such an approach has proved to be a useful tool/technique in characterizing the electrical nature of a number of heterogeneous systems [18-30]. This technique unravels the underlying competing phenomena via lumped parameter/complex plane analysis (LP/CPA). The total *ac* response of the material system can be modeled in terms of equivalent circuit elements which identifies conduction mechanisms in an operating electrical path between the electrode terminals. Based on the slope of the straight line of the Bode plots and the semicircular relaxation of the complex plane plots Debye and non-Debye responses can be delineated. Nevertheless, the elements of an equivalent circuit model can be related to the charge carrying species.

In this work, the *sterile BHI* (hereafter *BHI*) and *E. Coli bacteria-suspended BHI* (hereafter *E. Coli*) are investigated using *ac* small-signal electrical measurements. Time dependence of these material systems is also investigated. These data are analyzed via complex plane formalisms as well as conventional Bode plot. From these plots it is revealed that the *R-C* series combination is shunted to support the non-blocking nature of the *dc* operative path of these material systems. Thus, the existence of the shunt resistor is verified for the sterile *BHI* and *E. Coli*.

The development of the correct equivalent circuit representation of both *BHI* and *E. Coli* systems is the underlying objective in this investigation. Distinction between Debye and non-Debye responses obtained from the complex plane formalisms in conjunction with the Bode plots is not included in this work. This is because the correct representation of the equivalent circuit model is addressed which is derived from the measured data. The Bode plot alone does not provide obvious understanding upon visual inspection whether it represents Debye or non-Debye response unless the slope of the straight line therein is determined. In this way the equivalent circuit presented in

this work is not the same as seen elsewhere [5-14]. Often *R-C* series circuit is extracted from the Bode plot as a final equivalent circuit model of this material system. That is why the correct representation of the equivalent circuit model is addressed which is derived from the measured data. In this way the equivalent circuit presented herein is not the same as seen elsewhere [5-14].

## Experimental

### (a) Escherichia Coli (E. Coli) cultures and media

The bacteria used were from a non-pathogenic *E. Coli* culture obtained from American Type Culture Collection (ATCC 8739) in Manassas, Virginia. The cultures were activated in a manner similar to Mason and Powelson [31] by first transferring the bacterial inoculum from a refrigerated slant to tryptic soy agar (TSA - Difco, Sparks, MD) plates and incubated at 37°C for 24h. A well-isolated single colony forming unit (CFU) was inoculated into 100mL of brain heart infusion (BHI) broth (Difco, Sparks, MD) and incubated aerobically at 37°C. The bacteria were grown in a manner similar to Al-Qadiri *et al* [32] in BHI at 37°C and transferred every 24h for at least 3days prior to use. A 24h culture of 3μL was inoculated into 30mL of BHI in a culture tube equipped with stainless steel probes for electrical impedance measurements. Commercially dehydrated or concentrated media were used and reconstituted according to the manufacturer's directions.

### (b) Electrical measurements

In this study sterile BHI medium and the *E. Coli* were used in the acquisition of the immittance data applying *ac small-signal* voltage (1 V peak-to-peak). Two identical sterile BHI samples in test tubes were used for this purpose. One used as the sterile BHI sample for which the measurement was noted as zero time. The other BHI contained suspended *E. Coli* for which the measurement was noted at certain intervals after the introduction of the bacteria. Thus, the measurements were recorded at 180min, 390min, 600min, 990min and 1440min.

Two electrodes inserted in the test tube were connected to the impedance analyzer (HP 4192A). The *ac small-signal* electrical data were obtained in the frequency range  $5\text{Hz} \leq f \leq 10\text{MHz}$ . These data were acquired in the admittance form ( $Y = G_p + j \omega C_p$ ) where  $G_p$  is the conductance,  $C_p$  is the capacitance ( $\omega \times C_p$  is the susceptance),  $\omega (= 2\pi f)$  is the angular frequency, and  $j = \sqrt{-1}$ . The measurements were performed at room temperature in the vicinity of about 25°C. These data were analyzed via complex plane formalisms and used in the Bode plane representation.

## Results and Discussion

### (a) Representation of the measured data in the complex plane formalism

Figure 1 depicts the terminal *ac* electrical data in the admittance (*Y*) plane of the sterile BHI medium (in blue) as well as the growing bacteria suspended in the BHI medium. The observed relaxation is semicircular on both positive and negative domains of the *Y*-plane. This is identical to the behavior observed earlier in the solid-state system [33]. The negative domain is attributed to the inductive response of the material system as noted in the negative capacitance domain. The positive domain semicircle exhibits center below the

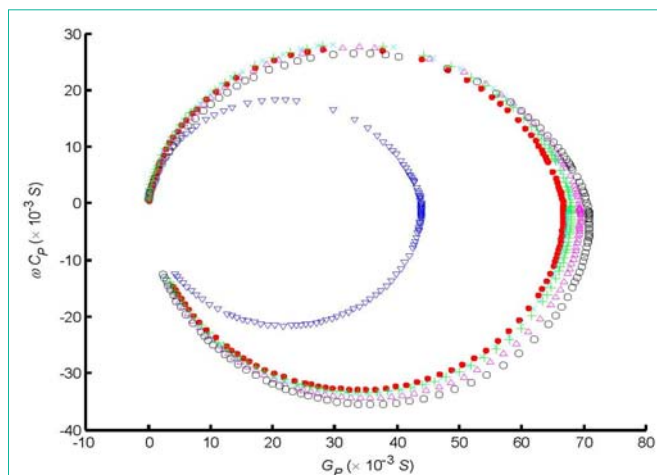


**Figure 1:** Measured data of the sterile BHI medium and *E. Coli* bacteria suspended in BHI medium in the *Y*-plane. Legend: ▽ - sterile BHI medium, *E. Coli* bacteria suspended in BHI medium after: • - 180 min, + - 390 min, x - 600 min, Δ - 990 min, and o - 1440 min.

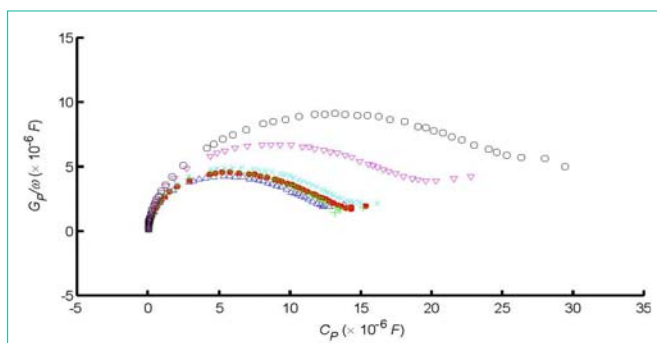


**Figure 2:** Measured data of the sterile BHI medium and *E. Coli* bacteria suspended in BHI medium in the *C*-plane. Legend: ▽ - sterile BHI medium, *E. Coli* bacteria suspended in BHI medium after: • - 180 min, + - 390 min, x - 600 min, Δ - 990 min, and o - 1440 min.

*x*-axis indicating depressed semicircle. Thus, each curve portrays non-Debye response of the material system as a whole. Overall, the conductance is increasing with time reflecting gradual multiplication of the *E. Coli* bacteria.

The same data when displayed in the complex capacitance plane (*C*-plane) shown in Figure 2 does not indicate straightforward semicircular loci. In this case a distorted semicircle appears indicating the presence of either Davidson-Cole [34, 35] (D-C) or Havriliak-Negami [36, 37] (H-N) type response. The skewed behavior of the semicircle in Figure 2 indeed yielded semicircular loci in Figure 1. The curves of Figure 2 indicate strong influence of the terminal conductance causing departure from the semicircular loci [26] is contribution of conductance is assessed as the skewed response resulting from the continued increase in the total *E. Coli* bacterial population. Similar response was noticed in a number of solid state materials and devices [15, 22-30].

### (b) Analysis of the data

The single non-Debye semicircular arc visible in the positive domain of the *Y*-plane shown in Figure 1 where frequency increases from left to right (clock-wise) can be displayed via the empirical relation:

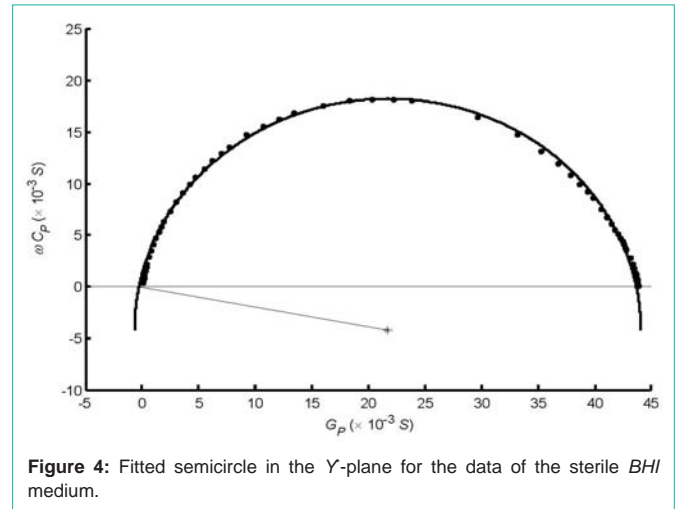
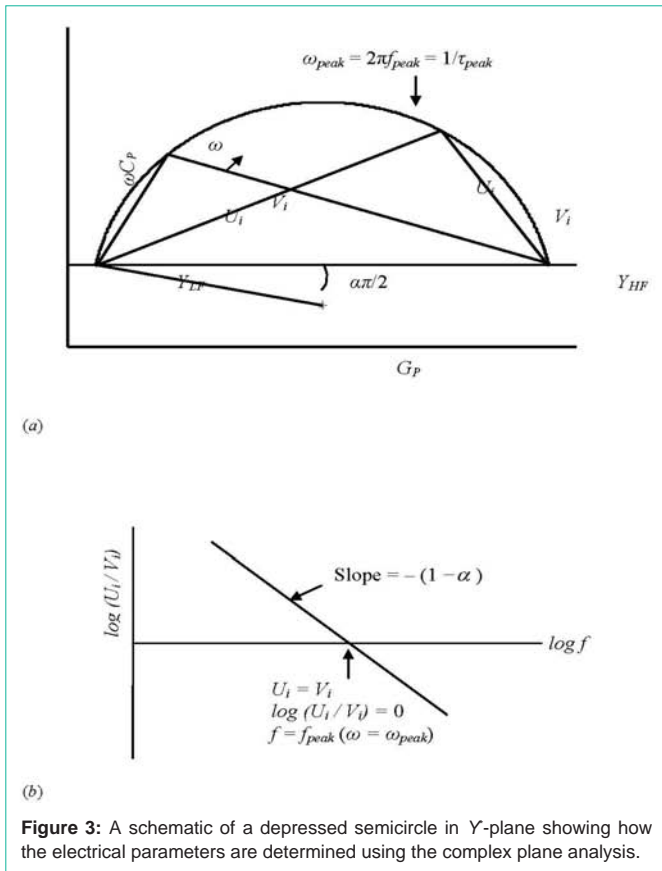


Figure 4: Fitted semicircle in the Y-plane for the data of the sterile BHI medium.

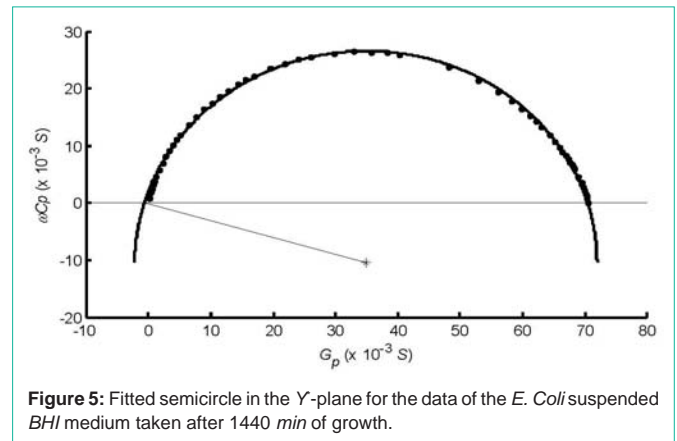


Figure 5: Fitted semicircle in the Y-plane for the data of the E. Coli suspended BHI medium taken after 1440 min of growth.

$$Y^*(\omega) = Y_{LF} + \frac{Y_{HF} - Y_{LF}}{1 + (j\omega\tau)^{1-\alpha}} \tag{1}$$

where  $Y_{LF}$  corresponds to low frequency (i.e.,  $f \rightarrow 0$ ),  $Y_{HF}$  corresponds to high frequency (i.e.,  $f \rightarrow \infty$ ),  $\tau$  is the relaxation time, and  $\alpha$  is the depression parameter related to the depression angle  $\theta$  as  $\theta = \alpha\pi/2$ . When the real part of equation (1) is plotted against the imaginary part, a semicircular locus is obtained with its center lying below the real axis referred to the depressed semicircle having non-Debye relaxation process. This is shown in generic form in Figure 3(a). To visualize the semicircle, both real and imaginary axes must be of the same grid-scale. The behavior turns Debye-like when  $\alpha \rightarrow 0$  and becomes highly non-Debye when  $\alpha \rightarrow 1$ .

The relaxation time  $\tau$  is determined from the frequency associated with the peak of the semicircle in a complex plane. This peak is the tangent of the semicircle that is parallel to the x-axis. Alternately, the tangent may be obtained from the mid-point of the diameter or the chord of the semicircle on the x-axis when drawn perpendicular that intersects the semicircular loci. The corresponding frequency is called the peak-frequency ( $f_{peak}$ ) used in determining the relaxation time via

$$\tau = \omega^{-1} = \omega_p^{-1} = \omega_{peak}^{-1} = \tau_{peak} = (2\pi f_{peak})^{-1} = (2\pi f_p)^{-1} \tag{2}$$

This is shown in Figure 3(a). The complex nonlinear least squares (CNLS) fitting of the semicircular behavior is used to extract the equivalent circuit parameters [15-17]. Necessary electrical parameters including left and right intercepts of a semicircular relaxation, relaxation time constant ( $\tau$ ) or angular peak-frequency ( $\omega_p = 2\pi f_p$ )

=  $1/\tau$ ), depression angle ( $\theta$ ), resistance and capacitance associated with the relaxation can be extracted using a complex nonlinear least squares (CNLS) curve fitting-software developed in authors' laboratory [38, 39]. This is demonstrated in Figure 3(b) and explained in reference [39].

Depending on the type of the complex plane, either the resistance or the capacitance of a semicircular relaxation should be independently extracted. Then the relaxation time ( $\tau = R \times C$ ) can be used to obtain the other equivalent circuit component. For example, in the Y-plane the time constant and its conductance component were obtained independently and then used to yield the associated capacitance according to the relation  $\tau = C/G$  where conductance  $G = 1/R$ .

Figure 4 shows the fitted semicircle for the sterile BHI whereas Figure 5 shows the same for E. Coli measured at 1440min after the start of the growth. These two figures reflect measurement frequency increasing clockwise direction. The growth of the bacteria is causing the increase of admittance between the two electrodes reflecting the decrease of resistance. Both fitted semicircles show the presence of a finite non-zero small left-side intercept which indicates a finite non-zero dc resistance. Both figures indicate the presence of non-Debye relaxation process as depicted by the depressed semicircles with finite depression parameter  $\alpha \approx 0.11$  for the sterile BHI and  $\alpha \approx 0.18$  for the E. Coli.

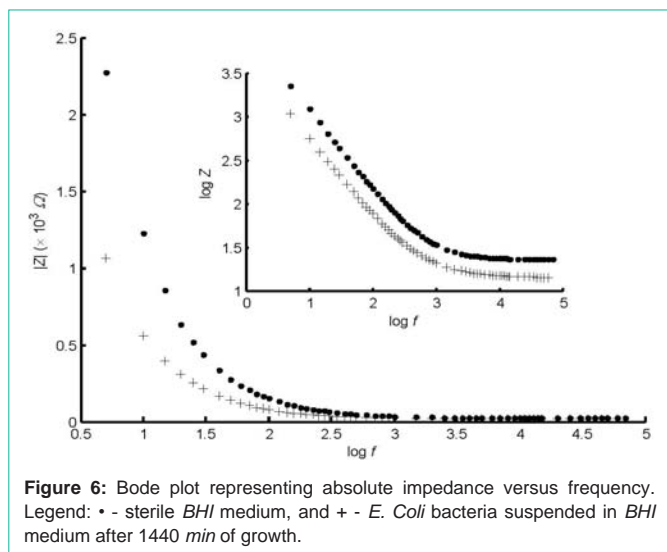


**Figure 6:** Bode plot representing absolute impedance versus frequency. Legend: • - sterile *BHI* medium, and + - *E. Coli* bacteria suspended in *BHI* medium after 1440 min of growth.

To further investigate the presence of the *dc* resistance, data are plotted in the  $C^*$ -plane as shown in Figure 2 where the frequency increases from right to left (anti-clockwise). As seen in this plot, each curve is skewed for the semicircular behavior and displays a highly non-Debye [26] and complicated relaxation process similar to either D-C or H-N process as noted earlier [34, 35]. The curves start deviating asymptotically at low frequency indicating the effect of a non-zero *dc* resistance. The magnitude of the *dc* resistance is presumed to be small due to the nature of the skewed behavior of each curve. Ideally a nearly vertical asymptotic behavior would have indicated the presence of a high value of the *dc* resistance. Therefore, both  $C^*$ - and  $Y^*$ -planes indicate the presence of a non-zero *dc* resistance.

Figure 6 shows Bode plot for the base (sterile) *BHI* medium identified at zero time, and the *E. Coli* measured at 1440min after the inclusion of the bacteria. The sterile *BHI* medium does not change significantly with time and not shown in the figure. The data taken after 390min for the *E. Coli* per Figure 1 exhibits smaller difference in conductance (i.e., larger resistance) with respect to the sterile *BHI* medium than the data taken after 1440min. The slope of the slant relaxation straight line in the log-log plot for the sterile *BHI* medium is  $-0.91$  [ $= -(1 - \alpha)$ ] and for the *E. Coli* is  $-0.81$  [ $= -(1 - \alpha)$ ]. These slopes indicate visible non-Debye response of both material systems. Invariably the *E. Coli* indicates higher degree of non-uniformity in the conduction process operative between the two electrodes than the sterile *BHI* medium. The depression parameter  $\alpha$  for the *BHI* sterile medium is 0.09 and for the *E. Coli* is 0.19. These two values are in good match for the respective response in the complex plane data fitting from Figures 4 and 5.

The CNLS fitting of the semicircular relaxation observed in the  $Y$ -plane via Figure 4 or 5 reveals relaxation time,  $\tau$ . It is related to the relaxation resistance ( $R_1$ ) and relaxation capacitance ( $C_1$ ) via the relation:  $\tau = R_1 \times C_1$ . When the behavior is perfectly Debye, the center of the semicircle lies on the real axis and the diameter of the circle is equal to the relaxation conductance, i.e. the reciprocal of  $R_1$ . When the behavior is non-Debye as observed in Figures 4 and 5, the relaxation resistance and capacitance are related to the chord of the semicircle as:

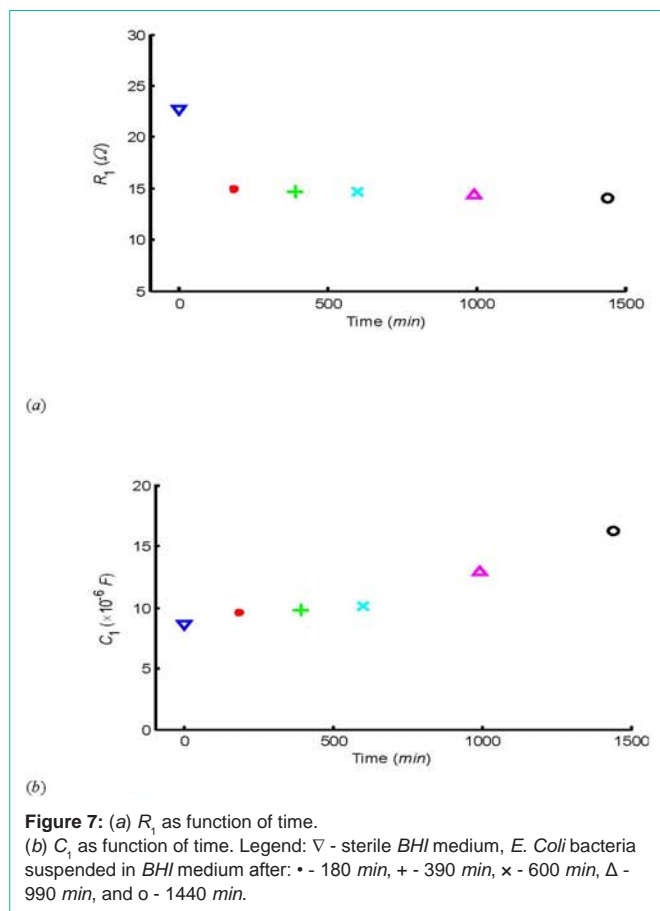


**Figure 7:** (a)  $R_1$  as function of time. (b)  $C_1$  as function of time. Legend:  $\nabla$  - sterile *BHI* medium, *E. Coli* bacteria suspended in *BHI* medium after: • - 180 min, + - 390 min, x - 600 min,  $\Delta$  - 990 min, and o - 1440 min.

$$R_1 = (Y_{HF} - Y_{LF})^{-1}, \quad \text{and} \quad C_1 = \tau / R_1. \quad (3)$$

To find the effect of the growth of *E. Coli* bacteria on the relaxation characteristics of the *BHI* medium, the following four parameters are calculated from the measured data at various time intervals:  $R_1$ ,  $C_1$ ,  $\tau$  and  $\theta$ . Figure 7 shows the variation of  $R_1$  and  $C_1$  with respect to time whereas Figure 8 shows the variation of  $\tau$  and  $\theta$ . The depression angle  $\theta$  slightly increases with time indicating non-uniformity in the susceptance reflecting capacitance of both sterile *BHI* and *E. Coli* material systems.

The relaxation behavior of the two distinguishable material systems has been observed in both  $C^-$  and  $Y^-$  planes in a simultaneous fashion. Better semicircular behavior is observed only in the latter plane whereas in the  $C^-$  plane the response is skewed indicating the influence of the *dc* conductance. This observation is similar to a number of polycrystalline solid state materials [15, 22-30]. Indeed such a response for the sterile *BHI* and *E. Coli* cannot be ignored. The same *ac* small-signal electrical data did not exhibit semicircular behavior in the other two complex planes (impedance  $Z'$  and modulus  $M'$ ). Due to the nature of the equivalent circuit shown in Figure 9 the response in these complex planes appeared as near straight lines and not presented here. The relaxation behavior, thus, observed is taken into consideration for deriving the non-blocking equivalent circuit model.

**(c) Equivalent circuit representation**

The non-Debye equivalent circuit model developed from the Bode

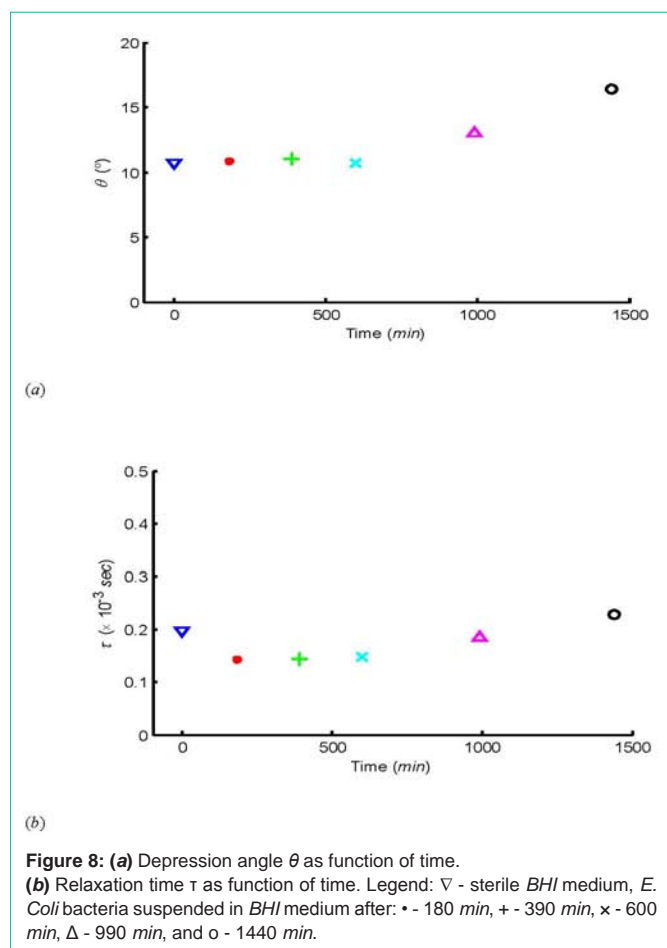


**Figure 8:** (a) Depression angle  $\theta$  as function of time. (b) Relaxation time  $\tau$  as function of time. Legend:  $\nabla$  - sterile BHI medium, *E. Coli* bacteria suspended in BHI medium after: + - 180 min, + - 390 min, x - 600 min,  $\Delta$  - 990 min, and o - 1440 min.

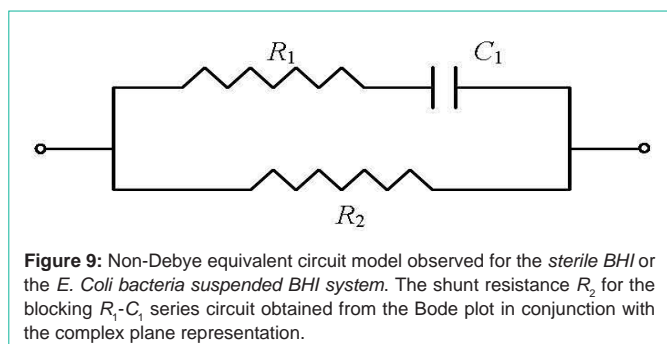


**Figure 9:** Non-Debye equivalent circuit model observed for the sterile BHI or the *E. Coli* bacteria suspended BHI system. The shunt resistance  $R_2$  for the blocking  $R_1$ - $C_1$  series circuit obtained from the Bode plot in conjunction with the complex plane representation.

plot in conjunction with the  $Y$ -plane as well as  $C$ -plane response is presented in Figure 9. This circuit is in strong agreement among these three representations of the same *ac* small-signal electrical data. In fact the resulting circuit is established by Grant [25] and verified for these samples. In the  $Y$ -plane relaxation, the CNLS curve fitting yielded a very tiny intercept on the left-side of the semicircle that substantiates the skewed response in the  $C$ -plane attributing to the presence of a *dc* conductance in parallel with  $R_1$ - $C_1$  combination extracted from the semicircular relaxation. The resistance  $R_1$  is extracted from horizontal straight line in the low frequency domain on the Bode plot shown in Figure 6 whereas the *dc* resistance denoted as  $R_2$  is extracted from the slant straight line obtained in the high frequency domain. The resistance  $R_1$  is extracted to be  $\approx 14 \Omega$  and  $R_2$  is extracted to be  $\approx 10^3 \Omega$  yielding match between the Bode plot and the complex plane representation.

The equivalent circuit model obtained in this study confirms the existence of a shunt resistance  $R_2$  for the blocking  $R_1$ - $C_1$  series circuit obtained from the  $C$ -plane or  $Y$ -plane relaxation. Such a situation verifies operative conductive path between the two electrodes. The shunt resistance (or conductance) is highly visible in the form of distorted or skewed semicircle at low frequencies in the  $C$ -plane. This kind of influence of the shunt resistance for the blocking  $R_1$ - $C_1$  circuit was demonstrated by Grant [29] and Coelho [40]. Invariably, the blocking nature is not existing either for the sterile BHI or the *E. Coli* bacteria suspended BHI system.

## Conclusion

This study confirms the existence of the operative shunt path for the blocking  $R$ - $C$  series circuit obtained from the Bode plot. The same finding is affirmed from the semicircular relaxation in the  $Y$ -plane. Therefore, sterile BHI or *E. Coli* bacteria suspended BHI always possess an overall non-blocking equivalent circuit model.

## References

1. Yang L, Li Y, Erf GF . Interdigitated Array microelectrode-based electrochemical impedance immunosensor for detection of Escherichia coli O157:H7. *Anal Chem.* 2004; 76: 1107-1113.
2. Felice CJ, Valentinuzzi ME . Medium and interface components in impedance microbiology. *IEEE Trans Biomed Eng.* 1999; 46: 1483-1487.
3. Yang L, Ruan C, Li Y . Detection of viable Salmonella typhimurium by impedance measurement of electrode capacitance and medium resistance. *Biosens Bioelectron.* 2003; 19: 495-502.
4. Yang L, Bashir R . Electrical/electrochemical impedance for rapid detection of foodborne pathogenic bacteria. *Biotechnol Adv.* 2008; 26: 135-150.
5. R. Gomez-Sjöberg and R. Bashir; "Impedance Microbiology-on-a-Chip: Microfluidic Bioprocessor for Rapid Detection of Bacterial Metabolism.," *Journal of Microelectromechanical Systems*, 14, 829-838 (2005).
6. R. Gomez, R. Bashir, and A. K. Bhunia; "Microscale Electronic Detection of Bacterial Metabolism," *Sensors and Actuators B*, 86, 198-208 (2002).
7. C. J. Felice, R. E. Madrid, J. M. Olivera, V. I. Rotger, and M. E. Valentinuzzi; "Impedance Microbiology: Quantification of Bacterial Content in Milk by Means of Capacitance Growth Curves," *Journal of Microbiological Methods*, 35, 37-42 (1999).
8. Yang L, Li Y, Griffis CL, Johnson MG . Interdigitated microelectrode (IME) impedance sensor for the detection of viable Salmonella typhimurium. *Biosens Bioelectron.* 2004; 19: 1139-1147.
9. J. Wu, Y. Ben, H.-C. Chang; "Particle Detection by Electrical Impedance Spectroscopy with Asymmetric-Polarization AC Electroosmotic Trapping," *Microfluid Nanofluid.* 1, 161-167 (2005).
10. S. Bayoudha, A. Othmaneb, L. Ponsonnet, and H. B. Ouadaa; "Electrical Detection and Characterization of Bacterial Adhesion using Electrochemical Impedance Spectroscopy-based Flow Chamber," *Colloids and Surfaces A: Physicochemical Eng. Aspects*, 318, 291-300 (2008).
11. R. Gomez, R. Bashir, A. Sarikaya, M. R. Ladisch, J. Sturgis, J. P. Robinson, et al.; "Microfluidic Biochip for Impedance Spectroscopy of Biological Species," *Biomedical Microdevices*, 3, 201-209 (2001).
12. Xiao C, Luong JH . Assessment of cytotoxicity by emerging impedance spectroscopy. *Toxicol Appl Pharmacol.* 2005; 206: 102-112.
13. C. Xiao, B. Lachance, G. Sunahara, and J. H. T. Luong; "Assessment of Cytotoxicity Using Electric Cell-Substrate Impedance Sensing: Concentration and Time Response Function Approach," *Analytical Chemistry*, 74, 5748-5753 (2002).
14. Y.-S. Liu, P. P. Banada, S. Bhattacharya, A. K. Bhunia, and R. Bashir; "Electrical Characterization of DNS Molecules in Solution Using Impedance Measurements," *Applied Physics Letters*, 92, 143902 (2008).

15. M. A. Alim; "Electrical Characterization of Engineering Materials," *Active and Passive Electronic Components*, 19, 139-169 (1996).
16. M. A. Alim; "Immittance Data-Handling/Analyzing Criteria for Heterogeneous Systems," in: *Materials Research Society Symposium Proceedings: Electrically Based Microstructural Characterization*, R. A. Gerhardt, S. R. Taylor, E. J. Garboczi edited, 411, 13-23 (1996).
17. M. A. Alim; "Phenomena Related to Concurrent Multiple Complex Plane Representations of the Immittance Data," *Materials Research Society Symposium Proceedings: Electrically-Based Microstructural Characterization*, R. A. Gerhardt, S. R. Taylor, E. J. Garboczi edited, 411, 113-122 (1996).
18. M. A. Alim, A. K. Batra, M. D. Aggarwal, J. R. Currie; "Immittance Response of the SnO<sub>2</sub>-Bi<sub>2</sub>O<sub>3</sub> Based Thick-Films," *Physica B*, 406; 1445-1452 (2011).
19. M. A. Alim, A. K. Batra, S. Bhattacharjee, M. D. Aggarwal; "Complex Capacitance in the Representation of Modulus of the Lithium Niobate Crystals," *Physica B*, 406; 1088-1095 (2011).
20. K. Batra, J. R. Currie, M. A. Alim, and M. D. Aggarwal; "Impedance Response of Polycrystalline Tungsten Oxide," *Journal of Physics and Chemistry of Solids*, 70, 1142-1145 (2009).
21. M. A. Alim, S. R. Bissell, A. A. Mobasher; "Analysis of the AC Electrical Data in the Davidson-Cole Dielectric Representation," *Physica B*, 403, 3040-3053 (2008).
22. A-. M. Azad, L. L. W. Shyan, and M. A. Alim; "Immittance Response of CaSnO<sub>3</sub> Prepared by Self-Heat-Sustained Reaction," *Journal of Materials Science*, 34, 1175-1187 (1999).
23. A-. M. Azad, L. L. W. Shyan, and M. A. Alim; "The AC Electrical Characterization of the Solid-State Reaction Derived CaSnO<sub>3</sub>," *Journal of Materials Science*, 34, 3375-3396 (1999).
24. C. C. Wang, V. D. Patton, S. A. Akbar, and M. A. Alim; "Effect of Zirconia Doping on the Electrical Behavior of Yttria," *Journal of Materials Research*, 11, 422-429 (1996).
25. C. C. Wang, W. H. Chen, S. A. Akbar, and M. A. Alim; "High-Temperature A.C. Electrical Behaviour of Polycrystalline Calcium Zirconate," *Journal of Materials Science*, 32, 2305- 2312 (1997).
26. M. A. Alim, M. A. Seitz, and R. W. Hirthe; "Complex Plane Analysis of Trapping Phenomena in Zinc Oxide Varistors," *Journal of Applied Physics*, 63, 2337-2345 (1988).
27. M. Hodge, M. D. Ingram, and A. R. West; "Impedance and Modulus Spectroscopy of Polycrystalline solid Electrolytes," *Journal of Electroanalytical Chemistry*, 74, 125-143 (1976).
28. M. Hodge, M. D. Ingram, and A. R. West; "New Method for Analyzing the ac Behavior of Polycrystalline Solid Electrolytes," *Journal of Electroanalytical Chemistry and Interfacial Electrochemistry*, 58, 429-432 (1975).
29. F. A. Grant; "Use of Complex Conductivity in the Representation of Dielectric Phenomena," *Journal of Applied Physics*, 29, 76-80 (1958).
30. M. A. Seitz; "Study of Heterogeneous Composite Materials via Lumped Parameter/Complex Plane Analysis," *International Journal of Hybrid Microelectronics (ISHM)*, 3, 1-7 (1980).
31. MASON DJ, POWELSON DM . Nuclear division as observed in live bacteria by a new technique. *J Bacteriol.* 1956; 71: 474-479.
32. H. M. Al-Qadiri, N. I. Al-Alami, M. Lin, M. Al-Holy, A. G. Cavinato, and B. A. Rasco; "Studying of the Bacterial Growth Phases using Fourier Transform Infrared Spectroscopy and Multivariate Analysis," *Journal Rapid Methods Automation Microbiology*, 16, 73-89, (2008).
33. M. A. Alim; "High-Frequency Terminal Resonance in ZnO-Bi<sub>2</sub>O<sub>3</sub>-Based Varistors," *Journal of Applied Physics*, 74, 5850-5853 (1993).
34. D. W. Davidson and R. H. Cole; "Dielectric Relaxation in Glycerine," *Journal of Chemical Physics*, 18, 1417-1417 (1950).
35. D. W. Davidson and R. H. Cole; "Dielectric Relaxation in Glycerol, Propylene Glycol, and n-Propanol," *Journal of Chemical Physics*, 19, 1484-1490 (1951).
36. S. Havriliak and S. Negami; "A Complex Plane Analysis of Dispersions in some Polymer Systems," *Journal of Polymer Science: Part C*, 14, 99-117 (1966).
37. S. Havriliak and S. Negami; "A Complex Plane Representation of Dielectric and Mechanical Relaxation Processes in some Polymers," *Polymer*, 8, 161-210 (1967).
38. M. A. Alim and S. Bhattacharjee; "Multi-Plane Immittance Data Analysis Software Package," Developed at the Alabama A & M University (2010).
39. W. Zhu, C. C. Wang, S. A. Akbar, A. Asiaie, P. K. Dutta, and M. A. Alim; "The AC Electrical Behavior of Hydrothermally Synthesized Barium Titanate Ceramics," *Japanese Journal of Applied Physics*, 35 Part 1, 6145-6152 (1996).
40. R. J. Coelho; *Physics of Dielectrics for the Engineer*, Elsevier Science, New York (1979).